From Observation to Simulation: Understanding Surprising Evolutions in Nova Ejecta

© F. Healy, T. J. O'Brien, R. Beswick, M. K. Argo

Jodrell Bank Centre for Astrophysics, University of Manchester, Manchester, United Kingdom

A classical nova occurs when a white dwarf (WD) in an interacting binary system undergoes a thermonuclear runaway (TNR) on its surface, leading to a large expulsion of material into the interstellar medium, as well as a dramatic optical brightening. Simple isothermal, spherically symmetric, homogeneous models for thermal radio emission from novae predict a light curve which brightens as t^2 (while the ejected shell is optically thick) and then declines as t^{-3} (once it becomes optically thin). However, observations of novae indicate that these models are flawed. For example, e-MERLIN, VLBI and VLA observations of Nova Mon 2012 have shown a complex, aspherical ejecta which evolves over time, whilst other studies have shown light curves which are not in agreement with the predictions of the models. In this talk we present new modelling of the radio emission from a variety of hypothesized ejecta structures. These models allow improved estimation of mass loss rate, which in turn tell us more about the mechanisms whereby the mass is lost, and allow us to investigate classical novae as possible Type 1a supernova progenitors. Developing an understanding of the geometry and possible collimation of the ejecta may also have implications for the study of particle acceleration in radio novae and similar systems.

Keywords: VLBI, Astrometry.

1 Introduction

A nova is a cataclysmic variable star consisting of a white dwarf (WD) and a main sequence, subgiant or red giant companion. In a nova explosion, the white dwarf undergoes a thermonuclear runaway (TNR) on its surface, as a result of build-up of accreted material from its companion. This leads to a large expulsion of matter from the WD surface, as well as a dramatic increase in the optical magnitude of the system. Novae usually expel between 10^{-7} $M_{\odot}$

and 10^{-4} $M_{\odot}$ of matter during an explosion, at velocities that can range from a few hundred km s^{-1}, to several thousand.

At radio frequencies, novae primarily emit due to thermal bremsstrahlung, although synchrotron radiation can also be detected if there are shocks present in the ejecta. Standard models of radio emission from novae (for example, the Hubble Flow model) predict an isothermal, smooth, spherically symmetric shell of expanding ejecta, with a light curve that increases as t^2 while the shell is optically thick, and a t^{-3} decay at late times once the source has become optically thin. However, some observations of novae indicate rather poor agreement with these simple models (see for example [10], [6], [7]).

1.1 V959 Mon

V959 Mon, also known as Nova Mon 2012, was first detected on June 19$^{\text{th}}$ 2012 by the Fermi Large Area Telescope, as a GeV γ-ray transient source ([1]), named J0639+0548. Shortly after this discovery, V959 Mon was obscured by the sun. Once V959 Mon became visible again, the γ-ray source was connected by [2] to an optical nova which was discovered in August 2012 by [5].

V959 Mon's discovery as a γ-ray source adds it to a growing list of classical novae that have been discovered to be γ-ray sources by the Fermi Large Area Telescope (see [4]). This recent spate of discoveries has been somewhat surprising, as the populations of relativistic particles required to produce GeV γ-rays had not been previously predicted in classical nova explosions.

EVN observations (made in September 2012) at 2–7 milliarcsecond (mas) resolution of V959 Mon at 5 GHz by [13] detected 2 compact components extending to the north-west and south-east, and moving apart with a proper motion of 0.45 milliarcseconds per day. Ongoing multi-frequency VLA observations of V959 Mon show a complex aspherical morphology, which appears to change in shape from an east-west elongation to a north-south elongation [3].

2 e-MERLIN Observations

The observations presented here were made with the e-MERLIN array over 6 epochs: September 18th 2012, November 12th 2012, November 22nd 2012, February 21st 2013, October 11th 2013 and February 21st 2014. All seven antennas in the array were used for the February 2013 and September 2012 observations; the Lovell telescope was omitted for the other epochs. The observations were made in the C Band(5.444–5.956 GHz for the first three epochs and 4.744–5.256 GHz for the last three epochs, with central frequencies of 5.7 GHz and 5 GHz respectively), providing a resolution of 40 milliarcseconds, and with a bandwidth of 512 MHz. The bandwidth was divided into

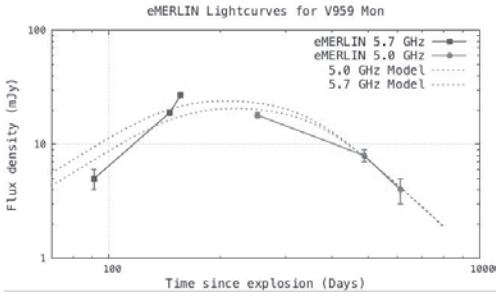

Fig. 1. e-MERLIN lightcurve for V959 Mon plotted alongside a model light curve calculated using the Hubble flow model, with distance $= 1.5$ kpc [12], electron temperature $= 2 \times 10^4$ K [3], outer velocity $= 2650$ km s^{-1}, and mass $= 1.5 \times 10^{-4}\ M_{\odot}$ (best-fit parameters returned by model fit to observations)

4 intermediate frequency bands (IFs), each containing 512 channels. The data were averaged such that each IF effectively contained 128 channels.

The calibration, reduction and imaging of each epoch was carried out with AIPS, using standard tasks. In all cases, J0645+0541 was observed as a phase calibrator, 3C286 as a flux calibrator and OQ208 as a band-pass calibrator. When imaging, a Briggs robustness parameter of 1 was used. The images were constructed using the different CLEAN restoring beams fitted to each one. They were then re-constructed using the same 70 mas $\times$ 70 mas circular beam for each epoch, so that the morphology could be more reliably compared from epoch to epoch.

The total flux of the source was measured at each epoch using the AIPS tasks JMFIT and TVSTAT. The fluxes are listed in Table 1. The e-MERLIN C-band lightcurve of V959 Mon is shown in Fig. 1. Also shown in that figure is a simulated lightcurve predicted for V959 Mon by the Hubble flow model. Using the best fit parameters to the VLA light curves as reported by [3], the model fitting program was given initial guesses of $4 \times 10^{-5} M_{\odot}$ for the ejecta mass, 2430 km s^{-1} for the outer velocity of the shell and 200 km s^{-1} for the inner velocity of the shell (recall that the Hubble flow model assumes an expanding spherical shell of ejecta). The distance to the nova (1.5 kpc, [12]) and the electron temperature of the ejecta (2×10^4 K, [3]) were fixed.

The model fitting program returned best fit parameters of $1.1 \times 10^{-4} M_{\odot}$ for the ejecta mass, 2300 km s^{-1} for the outer velocity of the shell and 470 km s^{-1} for the inner velocity of the shell; these values were reasonably consistent with those found by [3].

e-MERLIN images of V959 Mon are shown in Fig. 2. In the first three epochs, the ejecta can be seen expanding in the east-west direction. The east-west expansion continues in the fourth epoch (February 2013), however a hint of north-south structure can also be seen at this time. In the subsequent two

Table 1
Total integrated fluxes of V959 Mon for each image presented in this section

Epoch	Days Since Outburst	Total Flux, mJy
18th Sept 2012	91	8 ± 2
12th Nov 2012	146	31 ± 1
22nd Nov 2012	156	27 ± 1
26th Feb 2013	252	14 ± 1
11th Oct 2013	479	11 ± 3
21st Feb 2014	612	5 ± 1

epochs (October 2013 and February 2014), the visible ejecta is elongated in the north-south direction. This change in orientation was also observed with the VLA by [3].

It is clear from the images presented in Fig. 2 that standard models of nova ejecta, which assume a spherically symmetric outflow, are wrong. An alternative model suggested by [3] assumes an ejecta consisting of two perpendicular bi-polar components: a slower-moving component which is accelerated by transfer of energy from the orbiting binary system, and a faster-moving component accelerated by winds from the WD surface, and emanating primarily from the polar regions of the WD. The faster-moving wind-driven component would initially dominate radio images, before becoming optically thin, revealing the slower orbital driven component. At early times, shocks would occur at the interface between the components. In addition to explaining the changing ejecta morphology observed by e-MERLIN and the VLA, this model might also explain V959 Mon's emission of γ rays at early times.

3 Radio Emission Models

In order to investigate whether or not the model proposed by [3] provides a plausible explanation for the unusual morphology seen in V959 Mon's ejecta, we have simulated radio emission from a density distribution representative of the ejecta behaviour proposed by [3]. We have simulated a distribution consisting of two orthogonal bi-polar ejecta components, both with a density distribution of the following form (see [9]):

$$\rho(r) = \frac{M}{4\pi R r^2}\,, \tag{1}$$

where *M* is the mass of the component, *R* is its radius, and *r* is the radial distance (see Fig. 3 for a schematic). The opening angles of the components were set such that the sum of the opening angles of the two components would add up to 90°.

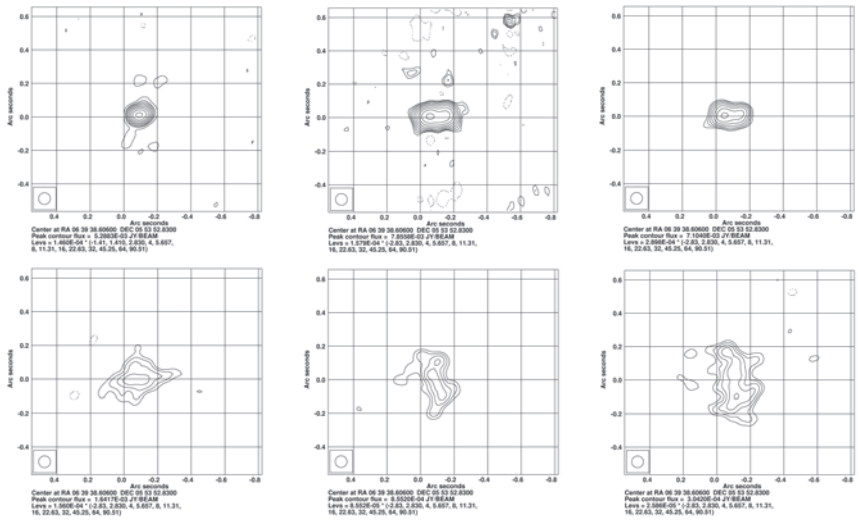

Fig. 2. Intensity contour plots of V959 Mon; from top-left: September 2012, 12th November 2012, 22nd November 2012, February 2013, October 2014, February 2014. The morphology can be seen to change from an east-west orientation, in the first four epochs, to what seems to be a north-south orientation, in the last two epochs. Each image was constructed using a 70×70 mas beam. The lowest contour level in each case is equal to three times the rms noise level (according to AIPS task IMSTAT) in the image

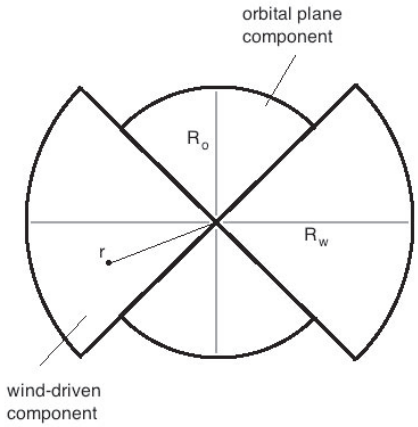

Fig. 3. Diagram of the morphology of the simulated radio emission. R_o is the radius of the orbital-plane component, and R_w is the radius of the wind-driven component

The radius of each component was evolved over time (by running the simulations for several different "epochs") to produce the expanding ejecta seen in the e-MERLIN observations. The east-west component (representing the fast "wind-driven" component predicted by [3]) was given a higher "expansion velocity" than the north-south "orbital plane" component (i. e. its radius was increased by a larger amount than that of the north-south component from epoch to epoch). The simulations were run for a range of ratios of north-south velocity to east-west velocity, from $v_{n-s} = 0.1 \times v_{e-w}$ to $v_{n-s} = 0.9 \times v_{e-w}$. The ratio of the masses of the two components was also allowed to vary; with the mass of the wind-driven component varying between 0.1 times and 0.9 times the total ejecta mass. The total mass of the ejecta was constrained at $1.1 \times 10^{-4} M_{\odot}$. The temperature of the ejecta was constrained at 10^4 K.

The simulations were run separately for the east-west "wind-driven" component, and the north-south "orbital plane" component. This allowed us to plot the contributions of the east-west and north-south components to the light curve separately, in order to see which of the components was dominating the total lightcurve over time. The simulations were run over 50 timesteps or "epochs", beginning on the day of the nova explosion (day 0) and continuing until 1000 days past the explosion.

The resulting light curves are shown in Fig. 4. As an initial step towards identifying which values for velocity ratio and mass ratio yield results which best match our observations of V959 Mon, we have considered two features of the simulated light curves.

Firstly, we have calculated residuals between normalized versions of the observed and simulated light curve, in order to identify which of the simulated light curves has the most similar shape to the observed light curve. We find values of $v_{n-s} = 0.7 v_{e-w}$ and $M_{n-s} = 0.7 M_{total}$ provide the best fit.

Secondly, we have studied the individual contributions made by the east-west/wind-driven component and the north-south/orbital-plane component to the total light curve, and identified which parameters yield light curves that are dominated at early times by the east-west component, and at later times by the north south component. By looking at the simulated light curves in this way, we find that the desired structure is produced when $v_{n-s} = 0.4 v_{e-w}$ or $0.5 v_{e-w}$ and $M_{n-s} = 0.4 M_{total}$ or $0.5 M_{total}$. The simulated radio images at epochs corresponding to the times when our observations were made are shown in Fig. 5.

Fig. 4. Simulated light curves of the two-component morphology outlined in this section, for a range of velocity and mass ratios between the two components. The light curves of the individual components are shown, as well as the total light curve of the system

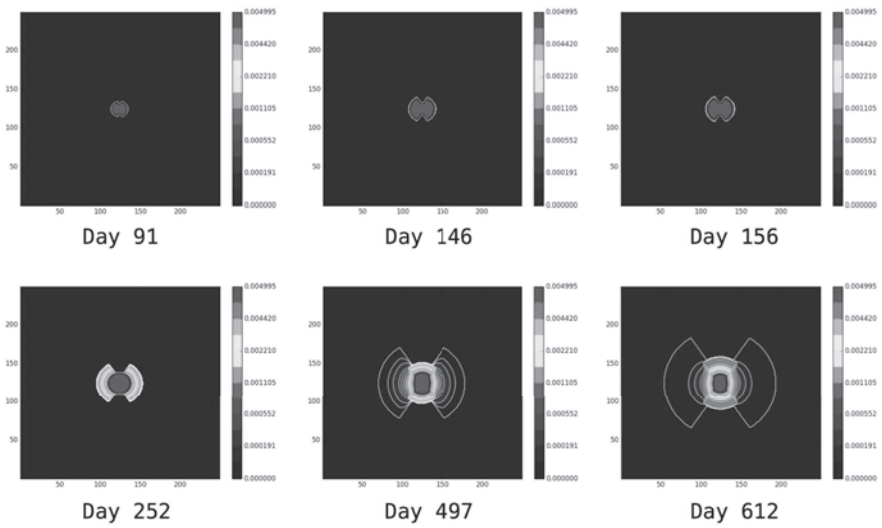

Fig. 5. Simulated radio images of the two-component morphology outlined in Section 3. The epochs shown here were chosen so as to match the actual days on which V959 Mon was observed by e-MERLIN

4 Conclusion

We have found that it is possible, using realistic values for the ejecta mass and temperature, to produce simulated emission which changes from being dominated by an east-west component to a north-south component over time, as a result of the faster east-west component becoming optically thin while the slower north-south component remains optically thick.

In order to properly compare the simulated images and light curves of nova ejecta presented here with the observed e-MERLIN data, it will be necessary to apply e-MERLIN UV coverage to the simulated emission. This will generate images which are a more accurate representation of what e-MERLIN could observe, and whose morphology can be compared directly with what is seen in the e-MERLIN images presented here.

However, the simulations presented here do not address the question of how such an ejecta structure could be generated, or whether or not the ejecta behaviour proposed by [3] is plausible. Alternative models which also seek to explain aspherical nova ejecta also exist. In order to answer these questions, and establish which model best explains why some novae display aspherical ejecta, it will be necessary to perform hydrodynamical simulations, with which we will attempt to determine how two orthogonal ejecta components might occur during nova outbursts. However, due to the increased computational power required for hydrodynamical modeling, it will be of use to have some constraints on quantities such as the ratio between the masses

of the two components, and their relative velocities. The more simplistic radio emission modeling we have outlined here will allow us to make estimates of such constraints.

References

1. *Cheung C. C. et al.* // The Astronomer's Telegram. — 2012. — 4224.
2. *Cheung C. C. et al.* // The Astronomer's Telegram. — 2012. — 4310.
3. *Chomiuk L., et al.* // Nature. — 2014. — 514(7522). — 339–342.
4. *Fermi-LAT Collaboration.* // Science. — 2014. — 345(6196). — 554–558.
5. *Fujikawa S., Yamaoka H., Nakano S.* Central Bureau Electronic Telegrams. — 2012. — 3202.
6. *Eyres S. P. S., Bode M. F., O'Brien T. J., Watson S. K., Davis R. J.* // Monthly Notices of the Royal Astronomical Society. — 2000. — 318(4). — 1086–1092.
7. *Heywood I., O'Brien T. J., Eyres S. P. S., Bode M. F., Davis R. J.* V723 Cas, Monthly Notices of the Royal Astronomical Society. — 2005. — 362(2). — 469–474.
8. *Hjellming R. M., Wade C. M., Vandenberg N. R., Newell R. T.* // The Astronomical Journal. — 1979. — 84. — 1619–1631.
9. *Hjellming R. A.* // The Physics of Classical Novae, ed. A. Cassatella, & R. Viotti. Berlin: Springer — 1990. — P. 169.
10. *Krauss M. I., et al.* // The Astrophysical Journal Letters 739.1. — 2011. — L6.
11. *Lloyd H. M., O'Brien T. J., Bode M. F.* // Monthly Notices of the Royal Astronomical Society. — 1997. — 284(1). — P. 137–147.
12. *Munari U., Dallaporta S., Castellani F., Valisa P., Frigo A., Chomiuk L., Ribeiro V. A. R. M.* // Monthly Notices of the Royal Astronomical Society, stt1340. — 2013.
13. *O'Brien T. J., et al.* // The Astronomer's Telegram. — 2012. — 4408. — 1.
14. *Osborne J. P., Beardmore A., Page K.* // The Astronomer's Telegram. — 2013. — 4727. — 1.
15. *Ribeiro V. A. R. M., Munari U., Valisa P.* // The Astrophysical Journal. — 2013. — 768(1). — 49.
16. *Wagner R. M., Woodward C. E., Starrfield S.* // The Astronomer's Telegram. — 2013. — 4737. — 1.